Vol. 30 (1999) ACTA PHYSICA POLONICA B No 7

B FACTORIES AND HERA-B PHYSICS POTENTIAL*

F. Sánchez

Deutsches Elektronen-Synchroton DESY
D-22603 Hamburg, Germany

(Received May 5, 1999)

CP-violation is one of the least understood phenomena in High Energy Physics. The observation of CP violation effects in B meson decays will allow stringent tests of the Standard Model to be made and may point the way to new physics. Many high-energy laboratories around the world have developed experimental programs to measure CP violation in the b sector and improve the knowledge in the b quark sector. This paper reviews the B-physics experiments that are currently being commissioned, focusing on the asymmetric e^+e^-colliders (BABAR and BELLE) and the fixed target experiment at DESY (HERA-B).

PACS numbers: 07.05.Fb, 12.15.Hh, 13.20.He, 13.65.+i

1. Introduction

The neutral B mesons are the only example — apart from neutral K and D mesons — of a particle which differs from its anti-particle only by a quantum number which is broken by weak interactions. This situation enables the second-order weak transitions between B^0 and $\bar{B}^0$, as observed in 1987 [1]. With this mixing, the $B^0\bar{B}^0$ opens the door for observing the second manifestation of the fundamental violation of CP invariance that was observed in the $K^0\bar{K}^0$ system [2].

Several challenging experiments are being constructed in order to search for this important symmetry violation. This paper will try to summarize the differences and similitudes of the different approaches and show the physics potential of the first generation of these experiments, the B-factories and HERA-B experiment.

This paper is organized in the following way: Section 2 reviews the framework of CP violation for B mesons, Section 3 describes the detectors

* Presented at the XXVII International Meeting on Fundamental Physics, Sierra Nevada, Granada, Spain, February 1–5, 1999.

that are currently being commissioned, Sections 4 will try to summarize the CP-violation and other physics potential and we summarize in Section 5.

2. The unitarity triangle and CP-violation

With the six observed quarks and six leptons, the weak Lagrangian is of the type current–current with the hadronic current given by:

$$J_\mu^{\mathrm{cc}} = \frac{e}{\sqrt{(2)}\sin\theta_\omega} \begin{pmatrix} \bar{u} & \bar{c} & \bar{t} \end{pmatrix}_L \gamma_\mu V_{\mathrm{CKM}} \begin{pmatrix} d \\ s \\ b \end{pmatrix}_L ,$$

$$V_{\mathrm{CKM}} = \begin{pmatrix} V_{ud} & V_{us} & V_{ub} \\ V_{cd} & V_{cs} & V_{cb} \\ V_{td} & V_{ts} & V_{tb} \end{pmatrix} .$$

The Cabbibo–Kobayashi–Maskawa matrix (V_{CKM}) reflects the fact that the physical states (mass eigenstates) and weak eigenstates are not the same. The actual knowledge of the CKM elements constrain in the absolute values, [4],

$$\begin{pmatrix} 0.9745-9760 & 0.217-0.224 & 0.0018-0.0045 \\ 0.217-0.224 & 0.9737-0.9753 & 0.036-0.042 \\ 0.004-0.013 & 0.035-0.042 & 0.9991-0.9994 \end{pmatrix} .$$

The fact that $|V_{us}| \approx 0.22 \gg |V_{cb}| \approx 0.04 \gg |V_{ub}| \approx 0.003$ permits to describe the CKM matrix in a form suggested by Wolfenstein [3] with four real parameters,

$$\begin{pmatrix} 1-\frac{\lambda^2}{2} & \lambda & A\lambda^3(\rho - i\eta) \\ -\lambda & 1-\frac{\lambda^2}{2} & A\lambda^2 \\ A\lambda^3(1-\rho-i\eta) & -A\lambda^2 & 1 \end{pmatrix} .$$

to the third order in λ, where $\lambda = V_{us} \approx -V_{cd} \approx 0.22$.

The CKM is a unitary matrix and its most general form may contain complex coefficients. If one applies the unitarity condition to the first and third columns of the CKM matrix one gets,

$$V_{ud}V_{ub}^* + V_{cd}V_{cb}^* + V_{td}V_{tb}^* = 0 .$$

This condition can be represented by a triangle in the complex space, the so-called unitarity triangle, see Fig. 1. The common phase is selected such that $V_{cd}V_{cb}^*$ lies in the horizontal plane. The triangle is re-scaled by a factor $|V_{cd}V_{cb}^*|$. CP-violation is possible when the elements $V_{ud}V_{ub}^*$ and

$V_{td}V_{tb}^*$ contain a non-zero imaginary phase. This condition is represented by a non-zero η parameter in the Wolfenstein parameterization. The goal of the new B experiments is to determine the sides and angles of the unitarity triangle.

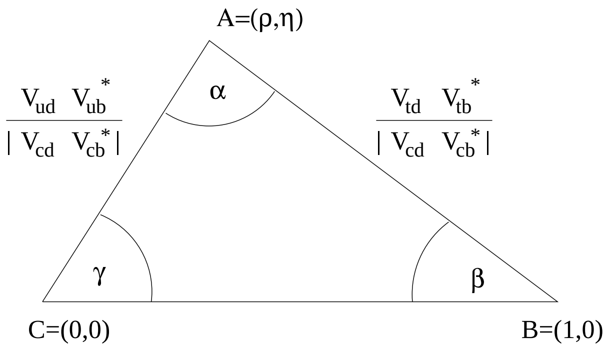

Fig. 1. Unitarity triangle in the complex space with the Wolfenstein parametrization.

In the neutral B meson system, the interference between the two competing amplitudes, Fig. 2, in the decay is expected to give the CP violating phase. Lets take the example of a decay to a CP eigenstate f and define the time integrated asymmetry as:

$$A_{\mathrm{CP}} = \frac{\Gamma(B^0 \to f) - \Gamma(\bar{B}^0 \to f)}{\Gamma(B^0 \to f) - \Gamma(\bar{B}^0 \to f)}\,.$$

To measure the angles β and α, the following asymmetries have been proposed:

$$A_{\mathrm{CP}}(B^0 \to J/\Psi K_S^0) = -\sin(2\beta)\frac{x_d}{1+x_d^2}\,,$$

$$A_{\mathrm{CP}}(B^0 \to \pi^+\pi^-) = -\sin(2\alpha)\frac{x_d}{1+x_d^2}\,,$$

where x_d is the $B^0\bar{B}^0$ oscillation frequency, and the α and β angles are defined in Fig. 1.

The decay of the B^0 meson into $J/\Psi K_S^0$ is generally considered the "golden" channel. The advantages of this channel arise from the very clean experimental signature and the small theoretical uncertainties. There is only one mixing process contributing to the decay (penguin diagrams are at the 2% level). The strong phase does not contribute to the asymmetry. The disadvantages come from the very low branching ratio of the decay channel: $BR(B^0 \to J/\Psi K_S^0) \approx 10^{-5}$. The CKM matrix elements contributing to the

Fig. 2. Decay of B^0 and $\bar{B}^0$ into a common state

decay are shown in Fig. 2. The product of the three amplitudes contributing to the decay:

$$\lambda = -\left(\frac{V_{tb}V_{td}^*}{V_{tb}^*V_{td}}\right)\left(\frac{V_{cs}^*V_{cb}}{V_{cs}V_{cb}^*}\right)\left(\frac{V_{cd}^*V_{cs}}{V_{cd}V_{cs}^*}\right)$$

carries the information about the angle β, $\mathrm{Im}\,\lambda = \sin 2\beta$.

The measurement of a second angle is of primary importance to constrain the unitarity triangle. The decay to $\pi^+\pi^-$ channel has been proposed by the new generation of experiments to measure the angle α . This decay channel has the disadvantage of being much harder to detect due to the large background and on the other hand the theoretical uncertainties are much larger than the ones of $J/\Psi K_S^0$ since there are different penguin diagrams phase contributing to the decay amplitude.

Fig. 3. CKM matrix elements contribution to the $B^0 \to J/\Psi K_S^0$ decay channel

3. B factories and HERA-B experiments

A measurement of CP violation in the B system requires a large sample of $B^0\bar{B}^0$ pairs. About 10^8 are needed to cope with the low "golden" channel branching ratio. Large B flavor tagging power and the capability to measure

B proper time are also needed to ensure the purity of the sample and be able to distinguish two B produced coherently. Flavor tagging requires K and lepton identification.

There are three ways of producing B hadrons in accelerators:

- e^+e^-annihilation at the $\Upsilon(4s)$ resonance with a cross-section of about 1 nb. This has been the approach of the DORIS storage ring at DESY with ARGUS detector and the CESR machine at Cornell with the CLEO detector. B mesons are produced as a decay product of the $\Upsilon(4s)$, as a consequence the B mesons are produced coherently ($B^0\bar{B}^0$, $B^-B^+, \ldots$ pairs) with the energy constrained by the machine energy.

  The new generation of experiments (BELLE-KEK, BABAR-PEPII) will produce boosted B mesons with asymmetric beams. This is essential to measure the difference of the decay time of the two B^0 mesons, which is needed to observe a CP-violation asymmetry.

- e^+e^-annihilation at the Z^0 pole with a cross-section of about 6 nb. B mesons are produced with a large boost such that the decay vertex can be reconstructed. In addition heavier mesons and Λ_B baryons are produced. The large sample accumulated by the LEP experiments at CERN and SLC at SLAC has been used to study lifetimes and time dependent oscillations.

- B production at Hadron machines: despite the large cross-section the huge background from inelastic collisions in proton machines prevented the development of B physics in this environment. Fix target experiments like HERA-B at DESY and pp colliders like CDF and D0 detectors at the Tevatron will compete in the next years with the e^+e^-colliders. CDF has already demonstrated the capabilities of the hadronic environment presenting the first measurement of the $\sin 2\beta$ angle [5]:

$$\sin 2\beta = 1.8 \pm 1.1 \pm 0.3\,.$$

To illustrate the differences between the $e^+e^-$and hadronic environments the main properties of the BABAR and HERA-B detector are shown in Table I.

In the future, dedicated experiments planned at the Large Hadron Collider (LHC) [9] and Tevatron [10] will address the measurement of CP violation with increased precision. This new generation of experiments will be able, by measuring the γ angle, to close the measurement of the unitarity triangle magnitudes.

TABLE I

Comparison of the main properties of BABAR and HERA-B detectors

	BABAR	HERA-B
$\gamma\tau c$	≈ 0.250 mm	≈ 10 mm
B vertex resolution	$\sigma_z \approx 0.080$ mm	$\sigma_z \approx 0.5$ mm
Impact parameter resolution	≈ 0.050 mm	≈ 0.050 mm
$< p_{B^0} >$	≈ 0.340 GeV	≈ 120 GeV
Mass resolution		
$J/\Psi K_S$	≈ 20 MeV	≈ 5.8 MeV
K_S	≈ 25 MeV	≈ 31 MeV
Track multiplicity	≈ 11	≈ 250 * 25 baryons 118 charged 131 neutrals

3.1. HERA-B detector

The HERA-B detector is located at the 920 GeV circulating proton beam of the HERA electron-proton collider at DESY. HERA-B is a fixed target experiment which is done by positioning 8 thin wires that interact with protons from the beam halo. In this mode it is able to run parasitically with the HERA collider experiments (ZEUS,H1 and HERMES).

The Hera-B detector, see Fig. 4 is a magnetic forward spectrometer covering 90% of the solid angle acceptance in the center-of-mass system. The main components of the detector are:

- a normal-conducting 2 Tm dipole magnet for momentum measurements.

- A silicon vertex detector with silicon strips for vertex reconstruction operated at 1 cm distance from the beam.

- tracking system. In order to keep occupancies below 20 % there are sections with different technologies and granularities. The system is divided into an outer part (honey-comb drift wire chambers with 5 and 10 mm cells) and an inner part (microstrip gas chambers with gas electron multiplication foils) and an innermost part consisting of silicon strip-detectors.

- three specialized gas-pixel chambers within the magnet provide additional information to trigger on High-p_T hadrons.
- A ring imaging Cherenkov counter to identify kaons. It uses C_4F_{10} as a radiator and multianode PMT as photosensitive devices.
- A transition radiation detector to improve electron identification at low angles using fiber radiators and straw tubes detectors.
- A W/Pb scintillator electromagnetic calorimeter.
- A muon detector with 4 layers of gas pad counters and pixel chamber at different depths in the absorber.

The performance of the different subdetectors is summarized in Table II.

The small signal to background ratio makes the HERA-B first-level trigger system one of the most challenging detector components. The first-level trigger hardware combines the lepton candidates from muon chambers and electromagnetic calorimeter with hits in four tracking layers, determines the momenta by imposing a rough vertex constrain and finally cuts on the invariant masses.(J/Ψ mass in case of dilepton and B^0 in case of the high-p_T

Fig. 4. HERA-B detector

TABLE II

Performance of the different HERA-B subdetectors

Detector	Performance
Vertex detector	$\sigma \approx 30\mu\mathrm{m}/p_t \oplus 25\mu\mathrm{m}$
inner tracker (6-19 cm)	$\frac{\sigma_p}{p} \approx 0.40\% \oplus 0.002\% p$
outer tracker (>19cm)	$\frac{\sigma_p}{p} \approx 0.50\% \oplus 0.005\% p$
RICH	$\pi - K$ misid. $< 2\%$ Eff $\approx 90\%$
TRD	$h - e$ misid. $< 7\%$ Eff $\approx 98\%$
EM calorimeter	$\frac{\sigma_E}{E} = \frac{17.0\%}{\sqrt{E}} \oplus 1.6\%$ inner
	$\frac{\sigma_E}{E} = \frac{9.5\%}{\sqrt{E}} \oplus 1.0\%$ outer
[2mm]Muon System	$\pi - \mu$ misid. $< 0.3\%$ @ 30 GeV

dipion trigger). The first level trigger input rate is 10 MHz, and provides a reduction factor of around 200. The trigger is refined in the high level software triggers to reduce them to 50 Hz logging rate.

The detector and trigger is described in more detail in [6].

3.2. BABAR and BELLE detectors

PEP-II is an asymmetric e^+e^-collider with beam energies of 9 GeV electrons against 3.1 GeV protons. The asymmetry gives a boost of $\beta\gamma = 0.56$ (*i.e.* $\gamma c\tau = 250$ μm for B^0 mesons). The design luminosity is $3 \times 10^{32}\mathrm{cm}^{-2}\mathrm{s}^{-1}$. The KEKB facility at KEK, collides 8 GeV electrons against 3.5 GeV positrons, leading to a boost of $\beta\gamma = 0.42$ (*i.e.* $\gamma c\tau = 200\mu$m for B^0 mesons) and a design luminosity of $10^{33}\mathrm{cm}^{-2}\mathrm{s}^{-1}$.

The detector at the two B factories are shown in Figs 5 and 6. There are similarities in the silicon vertex detector, central tracking detector, the solenoid field, the CsI electromagnetic calorimeter and the muon detector. The main detector components are described in the following:

- BABAR (BELLE) Vertex detector consist of 5(3) layers of double-sided silicon microstrip detectors.

- The BABAR (BELLE) central drift chamber consist of 40(50) layers of axial and stereo wires. It measures the transverse momentum of charged tracks and provides dE/dx information for particle identification.

Fig. 5. BABAR detector

- The main difference is in the particle identification: in the BELLE detector is done by a combination of an aerogel Cherenkov counter and time-of-flight counters, while for the BABAR detector a novel Cherenkov counter is developed using quartz radiator and collecting internally reflected Cherenkov light (DIRC).

- The BABAR (BELLE) electromagnetic calorimeter consist of 7000 (6500) CsI crystal towers. The crystal length ranges from 16 to 17.5 X_0 in BABAR and it is fixed to 16.2 X_0 in BELLE.

- Both experiments have a superconducting solenoid that provides 1.5 T in the cylindrical volume.

- The muon detector is instrumented on the flux return that acts as an absorber. The BABAR (BELLE) active components consists of 17–18(14–15) planes of resistive plate chambers.

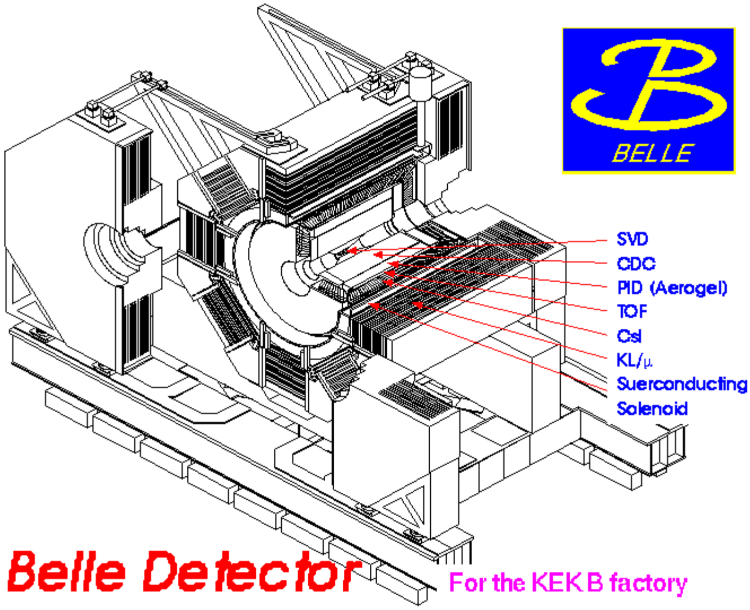

Fig. 6. BELLE detector

TABLE III

Performance of the different BABAR and BELLE subdetectors

Detector component	BABAR	BELLE
Vertex detector	$\sigma_{x,y,z} = \frac{50\mu\text{m}}{p} \oplus 15\mu\text{m}$ @ 90°	$\sigma_z = 100\mu\text{m}$
Drift chamber	$\frac{\sigma_{p_t}}{p_t} = 0.21\% + 0.14\% p_t$	$\frac{\sigma_{p_t}}{p_t} = 0.3\%\sqrt{1+p_t^2}$
Particle id.	$\geq 4\sigma K/\pi$ separation up to 3 GeV up to 3 GeV	$\geq 3\sigma K/\pi$ separation up to 3.5 GeV
Calorimeter	$\frac{\sigma_E}{E} = \frac{1.0\%}{\sqrt[4]{E}} \oplus 1.2\%$	$\frac{\sigma_E}{E} = \frac{0.67\%}{\sqrt{E}} \oplus 1.8\%$
Muon detector	$\pi - \mu$ misid. $\approx 5.0\%$	1% hadron fakes.

Table III summarizes the expected performance of the different BABAR and BELLE components.

The trigger has to rise to rather severe backgrounds from the accelerator, producing up to several kHz of interactions with two or more tracks reaching the calorimeter. The trigger consists mainly of a main (Level 1) trigger followed by a software trigger running on a CPU farm.

4. The physics potential

4.1. CP violation measurements

The three collaborations list quite a large number of channels that are to be used to study CP violation. Table IV summarizes these channels. The kinematic constraint in e^+e^-environment gives access to the $J/\Psi K_L^0$ channel. BABAR and BELLE can also reconstruct neutral pions and thereby $K_S^0 \to \pi^0\pi^0$ due to the clean e^+e^-environment.

TABLE IV

Comparison of decay channels used by HERA-B and BABAR/BELLE to measure CP violation in $B^0\bar{B}^0$.

CP angle	BABAR/BELLE	HERA-B
$\sin 2\beta$	$J/\Psi K_S$	$J/\Psi K_S$
	$J/\Psi K_L$	
	$J/\Psi K^*$	$J/\Psi K^*$
		$J/\Psi \rho$
	D^+D^-	
	$D^{*+}D^{*-}$	$D^{*+}D^{*-}$
	$\chi_{c1}K_S$	$\chi_{c1}K_S$
$\sin 2\alpha$	$\pi^+\pi^-$	$\pi^+\pi^-$
	$\pi^0\pi^0$	
	$\rho\pi$	
	$\pi^\mp a_1^\pm$	$\pi^\mp a_1^\pm$

The low background in e^+e^-collisions allows BABAR and BELLE to achieve better trigger and reconstruction efficiency than HERA-B. The trigger efficiencies are presented in Tables V and VI for the $J/\Psi K_S^0$ and $\pi^+\pi^-$ decay channels.

The main source of inefficiency in the BABAR charged $J/\Psi K_S^0$ reconstruction comes from tracks with low transverse momentum. The main source of inefficiencies in HERA-B arises from the K_S^0 reconstruction, where the K_S^0 has a median energy of 36 GeV and a considerable number of them decay inside and after the magnet and cannot be properly reconstructed. These trigger inefficiencies are compensated in HERA-B by the larger B^0 production cross section. In Table V a comparison of expected events and uncertainties after one year running at design luminosity are given. In the "golden" decay channel both experiments achieve similar measurement power. BABAR has studied other channels, mainly $J/\Psi K_L^0$, to achieve higher accuracy for β.

TABLE V

Comparison of trigger and reconstruction $J/\Psi K_S^0$ efficiency for BABAR and HERA-B and estimation of $\Delta \sin 2\beta$.

$J/\Psi K_S^0$	BABAR	HERA-B
Trigger	100%	53%
Charged reconstruction	59%	22%
Neutral reconstruction	35%	no estimation
Total Efficiency	52%	8%
Events (1 year at design luminosity)	1100	1400
$\Delta \sin 2\beta$	0.10	0.13
Other Channels		
$\Delta \sin 2\beta$ all channels	0.06	no estimation

TABLE VI

Comparison of trigger and reconstruction $\pi^+\pi^-$ efficiency for BABAR and HERA-B and estimation of $\Delta \sin 2\alpha$. HERA-B quotes $\Delta \sin 2\alpha$ as a function of the Background to signal ratio (χ).

$\pi^+\pi^-$	BABAR	HERA-B
Total trigger efficiency	$\approx 100\%$	19%
Events (1 year at design luminosity)	400	850
$\Delta \sin 2\alpha$	0.20	$0.14\sqrt{1+\chi}$ $(0.20\ \chi = 1)$
Other Channels		
$\Delta \sin 2\alpha$	0.11 $(\rho^{\pm}\pi^{\mp})$	$0.11\sqrt{1+\chi}$ $(a_1^{\pm}\pi^{\mp})$ $(0.16\ \chi = 1)$
$\Delta \sin 2\alpha$ all channels	0.10	0.12

The special high-p_t trigger is being built by the HERA-B collaboration for the very important $\pi^-\pi^+$ channel. The trigger has to cope with a very harsh background leading to a low trigger efficiency. An additional factor in the determination of $\sin\alpha$ arises from the ratio signal to background. The preliminary studies indicate that a ratio of less than one is achievable. The experimental conditions of BABAR are much cleaner, $\approx$ 100% efficiency, with a lower production cross section. It is important to note that both experiments achieve similar resolutions, see Table VI, and both propose additional channels to improve the measurement ($\rho\pi$ is accessible to BABAR because of π^0 reconstruction capabilities).

4.2. Other physics topics

The three collaborations have a large additional physics agenda. Table VII gives an overview. The experiments will profit from a large b and c quark sample to measure CKM matrix elements, B mixing, rare decays, $D\bar{D}$ mixing, ... HERA-B will be able to study J/Ψ and $b\bar{b}$ production for QCD studies, study b baryons properties, and look for rare b mesons like B_c. BABAR and BELLE will have access to a more diverse physics program with contributions to τ physics near the production threshold and $2-\gamma$ physics.

TABLE VII

Summary of the additional physics goals of HERA-B, BABAR and BELLE experiments

Physics topic	BABAR/BELLE	HERA-B
$B^0\bar{B}^0$ mixing	yes	yes
$B^0_s\bar{B}^0_s$ mixing	special $\Upsilon(5s)$ run	normal running, $x_s < 18.$
CKM		
V_{cb}	$B \to D^* l\nu$	$B \to D^* l\nu$
V_{ub}	$B \to X_u l\nu$ $X_u = \pi,\rho,\omega$	$B \to X_u l\nu$ $X_u = \pi,\rho,\omega$
V_{ts}	$\frac{B\to\rho\gamma}{B\to K^*\gamma}$	B_s mixing
Rare B decays	yes	yes (look for B_c state)
B baryons	no	lifetime, polarization, CKM, ...
τ physics	yes	no
$2-\gamma$ physics	yes	no
$D\bar{D}$ mixing	yes	yes

5. Summary

CP violation in the B-system will be studied in the near future by the B-factories and the HERA-B experiment. All the experiments are under construction and commission and will start the physics program around year 2000. The different source of systematic errors will provide independent measurements and will allow checks of the consistency of the Standard Model and studies of the source of the CP violating phenomena.

The main challenges of the BABAR and BELLE experiments will be to provide the design luminosity while keeping the machine background low. The background will affect the performance and lifetime of silicon vertex detectors and could blind the trigger increasing detector occupancies.

The challenge for HERA-B is to commission the detector and trigger performance under large background to signal ratio environment similar to the LHC experimental conditions. The radiation hardness of the different subdetectors and the large detector occupancies are the main issues for the collaboration.

There is a large number of topics beyond the CP violation measurement. The physics program does not completely overlap, such that the experimental situation in the B-sector will favorably improve.

We should not forget the CDF and D0 detectors at the Tevatron, upgrades of the detectors and a larger luminosity will open the possibility of competing in the measurement of $\sin 2\beta$ as it has been recently proven [5].

B physics will not stop at this generation of experiments. A new generation is under preparation at CERN (LHC-B) [9] and Fermilab (B-TEV) [10]. The increasing precision of these new detectors will allow a better understanding of CKM matrix and will allow to search look for deviations of standard model at the level of 1%.

REFERENCES

[1] H. Albrecht *et al., Phys. Lett.* **192B**, 245 (1987).

[2] J.H. Christenson, J.W. Cronin, V.L. Fitch, R. Turlay. *Phys. Rev. Lett.* **97**, 1387 (1955).

[3] L. Wolfenstein, *Phys. Rev. Lett.* **51**, 145 (1983).

[4] C. Caso *et al.*, *Eur. Phys. J.* **C3**, 1–794 (1998).

[5] F. Abe *et al.*, *Phys. Rev. Lett.* **51**, 81, 5513 (1998).

[6] E. Hartouni *et al.*, DESY-PRC 95/01, 1995; T. Lohse *et al.*, DESY-PRC 94/02, 1994; H. Albrecht *et al.*, DESY-PRC 92/04, 1992.

[7] The BELLE collaboration, KEK report 95-1, April 1995.

[8] D. Boutigny *et al.*, SLAC-R-95-457,1995.

[9] T. Nakada, *Acta Phys. Pol.* **B30**, 2433 (1999).

[10] P. Casper, *Nucl. Instrum. Methods Phys. Res.* **A408**, 146–153 (1998).